Organic molecules on zirconium surfaces

N. Stojilovic and R. D. Ramsier[a)]
Departments of Physics, Chemistry, and Chemical Engineering, The University of Akron, Akron, Ohio 44325

(Received 9 October 2003; accepted 1 March 2004; published 21 July 2004)

In this work, the behavior of Zr(0001) exposed to benzene (C_6H_6) and deuterated methanol (CD_3OD) is discussed. Relatively simple surface kinetics for the C_6H_6/Zr(0001) and CD_3OD/Zr(0001) systems are observed, with only molecular desorption detected in thermal desorption experiments. We attribute this to the presence of a passivating layer of carbon formed by the initial decomposition of these species on the reactive Zr(0001) surface. Following adsorption at 150 K, benzene desorbs at about 715 K, whereas methanol desorbs near 600 K. An increase in adsorption temperature of 20 K for C_6H_6 and of 10 K for CD_3OD lowers desorption yields significantly. An increase in surface oxygen is observed by Auger electron spectroscopy (AES) after exposure to benzene, possibly due to surface-carbon/subsurface-oxygen exchange. AES indicates that carbon stays in the near-surface region after thermal desorption, but that oxygen diffuses into the bulk in both cases. © *2004 American Vacuum Society.* [DOI: 10.1116/1.1723308]

I. INTRODUCTION

Zirconium can take relatively large quantities of various atoms into solid solution, and, upon heating, these dissolved atoms may return to the surface and participate in surface processes. When this happens, it usually makes analysis of thermal desorption kinetics very difficult. It is known that high-temperature annealing causes oxygen and carbon diffusion into the bulk,[1] but on the other hand, induces sulfur segregation to the surface.[2] It has also been observed that surface oxygen enhances the segregation of bulk hydrogen to zirconium surfaces.[3,4] Results from our laboratory, involving nitrogen- and oxygen-containing species,[5,6] also demonstrate the complex surface chemistry of this metal. For example, Zr(0001) exposure to both ammonia and nitric oxide results in the thermal desorption of water and a strong dependence of the desorption peak temperature on adsorption temperature.[6] Even though some impurity carbon was present in these previous studies, it did not prevent surface-bulk diffusion and exchange of oxygen and nitrogen.

One of our goals is to gain a better understanding of this surface-bulk diffusion and of the involvement of impurity atoms in surface kinetics on zirconium surfaces. In the present effort, we investigate zirconium surface chemistry when carbon is present by exposing Zr(0001) surfaces to organic molecules. We have chosen C_6H_6 and CD_3OD as probe species in this case. We will discuss the similarities between the C_6H_6/Zr(0001) and CD_3OD/Zr(0001) systems and compare our findings with those for nitrogen-containing molecules on Zr(0001) surfaces.

II. EXPERIMENTAL DETAILS

The Zr(0001) single crystal used in these studies is a cylindrical disk polished on one side to 0.03 μm with uncertainty in orientation of less than 1°. The crystal is 1 mm thick and has a 3 mm radius. Two type-E thermocouples are spot-welded to the sample and are part of a temperature-controlled feedback loop. Two tantalum wires are also spot-welded to the sample, providing dc heating. The sample is cooled by a copper braid attached to a liquid-nitrogen cold finger. The stainless steel UHV system used in these experiments is pumped by a turbomolecular pump, an ion getter pump, and a titanium sublimation pump together with a liquid-nitrogen-cooled cold trap. The chamber is equipped with a quadruple mass spectrometer and retarding-field Auger electron spectroscopy (AES)/reverse-view low-energy electron diffraction (LEED) optics. More detailed descriptions of the chamber are available elsewhere.[7,8]

Cleaning the sample of residual carbon after exposure to benzene and methanol requires repeated sputtering–annealing cycles. For sputtering, Ar (99.9999%, 2 keV, 2 μA cm^{-2}) ion bombardment at $\sim 3\times10^{-6}$ Torr is used. Following sputtering, the sample is then annealed to 840 K for 2 min. The cleanliness of the sample is monitored by AES, with carbon and oxygen surface contaminants kept at our previously reported ''clean'' surface levels.[9]

Following backfilling of the chamber, all experiments are conducted at or below a base pressure of $\sim 3\times10^{-10}$ Torr. Liquid benzene (C_6H_6, 99.0%) and methanol (CD_3OD, 99.8%) are used as sources for the backfilling gases. Several freeze–pump–thaw cycles are performed and the purities of both backfilling gases are monitored by mass spectrometry. The pressure during backfilling is controlled by a precision leak valve and is kept at $\sim 3\times10^{-8}$ Torr. Exposures are expressed in Langmuir ($1\ L = 10^{-6}$ Torr s) units, with no correction for ion-gauge sensitivity.

Temperature-programmed desorption (TPD) as well as stepwise annealing experiments are conducted with a heating rate of 1.8 K/s, with AES spectra taken after cooling the sample down to 150 K. Additionally for C_6H_6/Zr(0001), the structures of adsorbed layers are probed by LEED (60 eV, 2 μA cm^{-2}). These experiments are also performed in stepwise annealing fashion at the same heating rate, with LEED images recorded digitally at 150 K.

a)Electronic mail: rex@uakron.edu

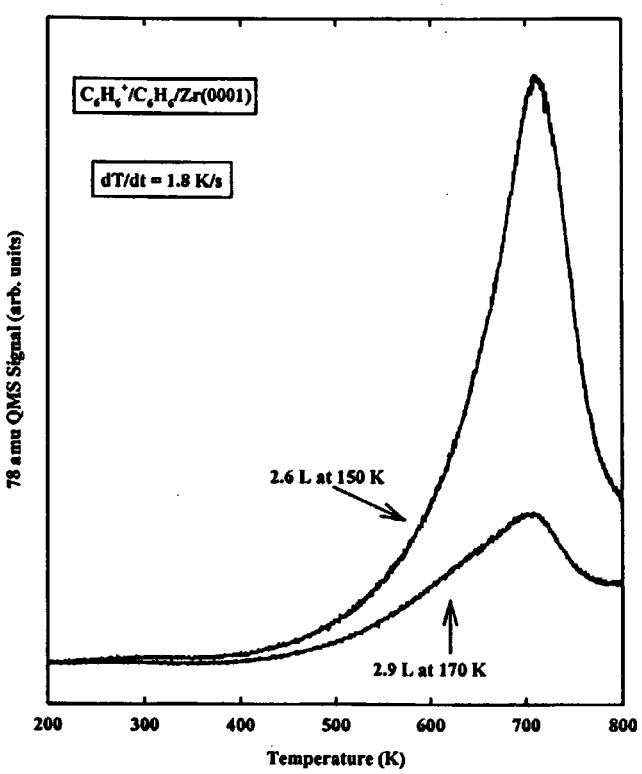

FIG. 1. $C_6H_6^+$ TPD spectra following exposure of Zr(0001) to benzene: 2.6 L at 150 K and 2.9 L at 170 K.

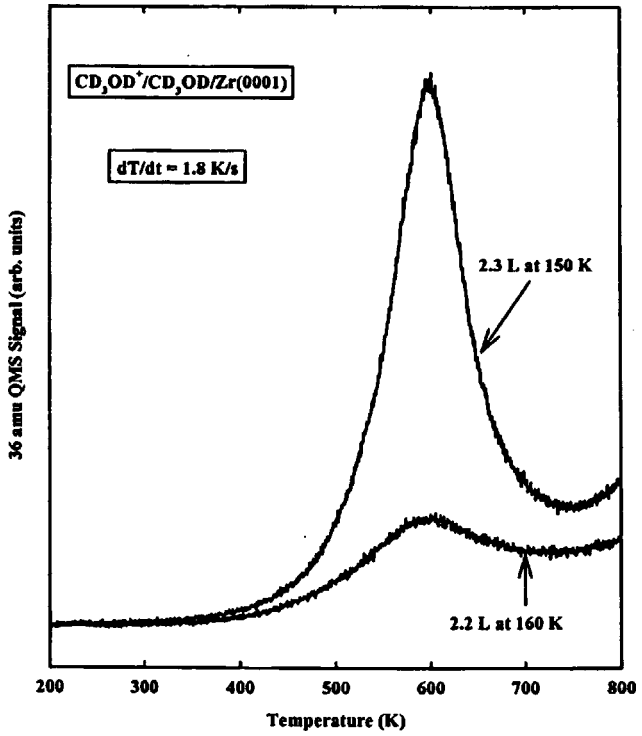

FIG. 2. CD_3OD^+ TPD spectra following exposure of Zr(0001) to methanol: 2.3 L at 150 K and 2.2 L at 160 K.

III. RESULTS AND DISCUSSION

A. TPD

Figure 1 presents TPD spectra of $C_6H_6^+$ following exposure of Zr(0001) to C_6H_6 at two temperatures. Exposures of 2.6 L at 150 K and 2.9 L at 170 K are shown as examples. Regardless of adsorption temperature, benzene desorbs near 715 K. Note the difference in the amount of desorbing benzene for different adsorption temperatures. Slightly lower exposure to benzene results in significantly higher desorption yield due to lower adsorption temperature. Exposure at lower temperature is usually associated with a higher sticking coefficient with surfaces being less aggressive toward dissociation of adsorbed molecules.

Figure 2 shows methanol (CD_3OD) TPD spectra following exposures at 150 and 160 K. Regardless of adsorption temperature methanol thermally desorbs near 600 K. Approximately the same exposures at two different temperatures result in a significantly different amount of desorbing methanol. As in the case of benzene on Zr(0001), a lower adsorption temperature produces a higher desorption yield. Presumably a lower sticking coefficient at the higher adsorption temperature and the ability of Zr(0001) to dissociate adsorbed species are responsible for these observations.

Figures 1 and 2 are presented with the same vertical scales and similarities of the TPD spectra are apparent. Peak profiles and heights are similar for similar exposures, and the amount of desorbing species is adsorption temperature dependent. Additionally, in both cases, the adsorbed molecules are the only desorbing species and desorption kinetics resemble those of first order. Changes in adsorption temperature have practically no effect on desorption temperature.

However, previous experiments on $NH_3/Zr(0001)$ and NO/Zr(0001)[6] reveal that higher adsorption temperatures result in higher desorption yields, opposite to what we observe for benzene and methanol on Zr(0001). Previously, it was also found that different adsorption temperatures resulted in different desorption peak temperatures for nitrogen-containing species. Finally, in addition to ammonia desorption from $NH_3/Zr(0001)$, the desorption of water is also detected, indicating participation of oxygen from beneath the surface. Therefore, the interaction of organic molecules with Zr(0001) is very different than for nitrogen-containing species, particularly NH_3 and NO.

Figure 3 shows C_6H_6 and CD_3OD integrated peak areas versus exposure following adsorption at 170 and 160 K, respectively. Relatively low exposures of up to 6 L are shown. Recall that exposure of Zr(0001) to benzene (Fig. 1) and methanol (Fig. 2) at higher adsorption temperature reduces desorption yield. However, Fig. 3 indicates that a 10 K higher adsorption temperature for benzene compared to that of methanol results in slightly greater TPD yields of benzene. This is probably the consequence of a greater sticking coefficient and stability of benzene on Zr(0001) compared to methanol.

Both C_6H_6 and CD_3OD exposures up to 1 L yield no thermal desorption peak, indicating dissociation of the first adsorbed layer(s). We are unable to determine whether dissociation occurs during adsorption or upon subsequent heat-

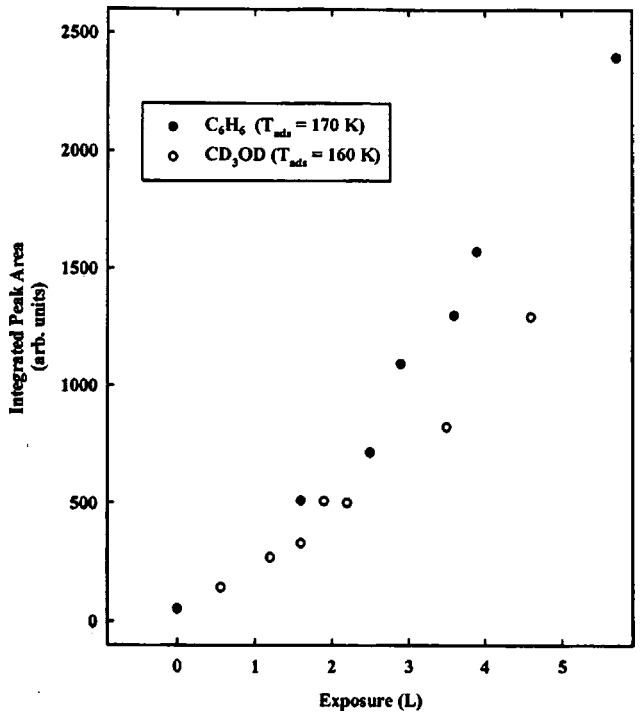

FIG. 3. Integrated desorption areas of benzene (solid points) and methanol (hollow points) from Zr(0001) surfaces following benzene adsorption at 170 K and methanol adsorption at 160 K, respectively.

ing, or the exact coverage. Our AES data (to be presented subsequently) for $C_6H_6/Zr(0001)$ show that exposures of less than 2 L result in an increased oxygen content on the surface. An exchange of carbon with subsurface oxygen is proposed to explain this result, which indicates that molecules most likely dissociate as they are adsorbed. This is consistent with the high reactivity of zirconium. Notice in Fig. 3 that the integrated peak areas increase monotonically with exposure, and no saturation in thermal desorption is observed. It should be noted that for ammonia[6,9] and nitric oxide[6,8] relatively high exposures of more than 20 L are needed for well-defined desorption features to develop, whereas for benzene and methanol, much lower exposures are needed.

B. AES

Figure 4 presents derivative-mode Auger electron spectra of $C_6H_6/Zr(0001)$. All measurements are taken after stepwise annealing followed by cooling the crystal to 150 K. Figure 4 focuses on C(*KLL*, 272 eV) and O(*KLL*, 512 eV) Auger features. Note that even the cleaned surface contains some carbon and oxygen as a consequence of the gettering nature of zirconium. Exposure of Zr(0001) to 1.7 L of benzene does not seem to change the C(*KLL*) feature, but results in an increase in surface oxygen. Spectra for this relatively low exposure are shown since the increase in oxygen content is pronounced for exposures less than 2 L.

Even though no apparent increase in the C(*KLL*) feature is notable in Fig. 4, the C(*KLL*, 272 eV)/Zr(*MNN*, 94 eV) Auger peak-to-peak height ratio (not shown) increases since the

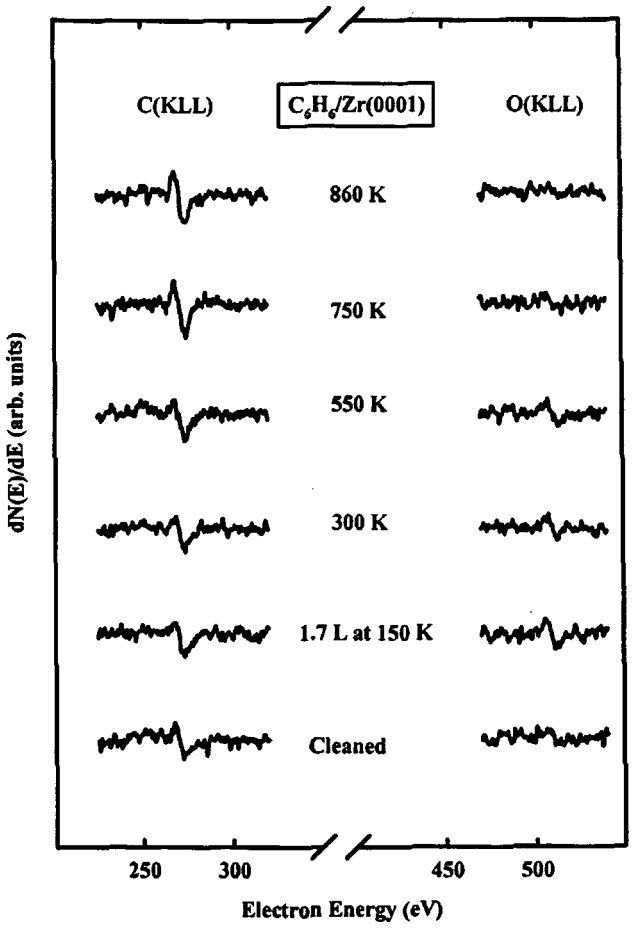

FIG. 4. Derivative-mode AES features of carbon (*KLL*, 272 eV) and oxygen (*KLL*, 512 eV) taken from $C_6H_6/Zr(0001)$ after stepwise annealing and then cooling the crystal down to 150 K.

Zr(*MNN*) feature is reduced due to electron attenuation caused by the adsorbates. On the other hand, an increase in surface oxygen is obvious in the actual spectra. For lower exposures very little or no thermal desorption of benzene is observed, and we propose that upon formation of the first adlayer(s), benzene dissociates and an exchange of surface carbon with subsurface oxygen occurs.

Carbon occupying sites beneath oxygen was also observed for CO on polycrystalline zirconium.[10]

Annealing to 550 K does not change the AES features of carbon and oxygen significantly, but further annealing to 750 and 860 K increases the C(*KLL*) and diminishes the O(*KLL*) Auger features. Since no desorption of oxygen-containing species is observed, the disappearance of the oxygen AES feature is attributed to oxygen diffusion into the crystal lattice. Note that unlike O(*KLL*), the C(*KLL*) feature is always detected in our experiments. This is due to the significantly slower diffusion rate of carbon into the bulk as compared to that of oxygen.[11]

Data in Fig. 5 are presented in a similar fashion to those in Fig. 4. Here, Auger electron spectra of $CD_3OD/Zr(0001)$ are shown for comparable annealing temperatures upon cooling the sample down to 150 K. The behavior is similar to that after benzene exposure. A larger carbon signal is observed

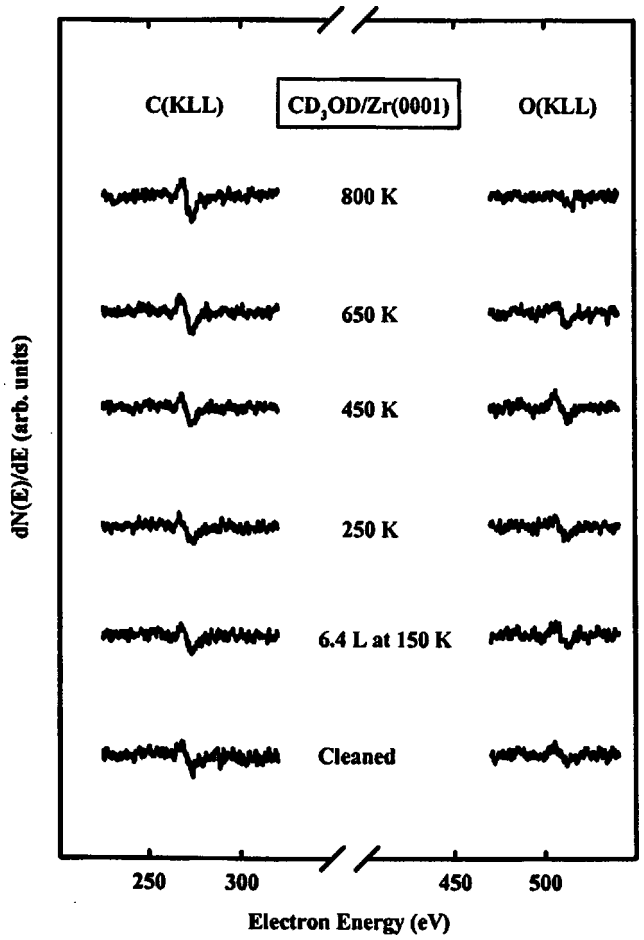

FIG. 5. Derivative-mode AES features of carbon (*KLL*, 272 eV) and oxygen (*KLL*, 512 eV) taken from $CD_3OD/Zr(0001)$ after stepwise annealing and then cooling the crystal down to 150 K.

following annealing to 650 or 800 K than immediately after exposure to methanol at 150 K. High-temperature annealing, like in the case of $C_6H_6/Zr(0001)$, causes diffusion of surface oxygen into the bulk.

C. LEED

No superstructure LEED patterns of $C_6H_6/Zr(0001)$ are observed for various exposures in the 1–6 L range and benzene adsorption results in only diffuse (1×1) patterns. It should be mentioned that other metals with the same surface structure, such as Ru(0001),[12,13] Os(0001),[14] and Co(0001)[15] all develop superstructure LEED patterns after exposure to C_6H_6. The response of Zr(0001) to adsorbed C_6H_6 obviously differs from these surfaces and is most likely a consequence of the reactive nature of zirconium and its ability to take large quantities of various atoms into solid solution. Presumably it is the presence of all three species, C, H, and O, that determines the structure of adsorbed layer. We should mention that there is a possibility of formation of a (1×1)-C structure as was observed for $C_2H_4/Zr(0001)$,[16] but we did not perform LEED intensity analysis to verify this.

D. Possible implications

Previous studies of other (non-carbon-containing) small molecules on Zr(0001) all indicate that dissociative adsorption is accompanied by surface/subsurface exchange and diffusion mechanisms which significantly influence the resulting surface chemistry. In those cases, oxygen, hydrogen, and nitrogen are considered to be mobile not only on the surface but within the subsurface regions, which results in strong temperature-dependent effects and complicated kinetics. The data we have thus far for carbon-containing species are consistent with this picture, in that:

(1) AES indicates an increase in oxygen at the surface following benzene adsorption that is pronounced at low exposures,
(2) very little desorption is observed at low exposures, and
(3) heating causes thermal desorption, after which the carbon content at the surface does not change significantly, whereas the oxygen content decreases.

All of these observations are indicative of dissociative adsorption and surface/subsurface exchange.

However, we propose that in the present cases, carbon essentially passivates the surface and/or increases the activation energy for subsequent diffusion of oxygen and hydrogen. This would explain why we observe relatively simple thermal desorption behavior with both methanol and benzene, as compared to ammonia, nitric oxide, water, and oxygen. By simple we mean that only molecular desorption is observed, that TPD yields can be understood with a simple sticking coefficient model, and that there is no strong dependence of desorption temperature on adsorption temperature. Thus, the present work implies that the behavior of subsurface species and impurity atoms cannot be neglected as we pursue a more quantitative understanding of the surface chemistry of zirconium.

IV. SUMMARY

In the present article we have discussed the interaction of benzene (C_6H_6) and methanol (CD_3OD) with Zr(0001). For exposures in the 150–170 K range, we find the thermal desorption kinetics of these two molecules to be very similar. Namely, there is no thermal production of new species, and the molecular desorption peak temperatures are unaffected by adsorption temperature for both systems. Higher adsorption temperatures result in lower desorption yields for both species. However, benzene desorbs at about 115 K higher temperature than methanol and with a slightly greater desorption yield. Oxygen diffuses into the bulk during annealing, whereas carbon stays in the near-surface region. For $C_6H_6/Zr(0001)$, an increase in oxygen content in the near-surface region is observed after adsorption, presumably reflecting surface-carbon/subsurface-oxygen exchange at low exposures. The presence of carbon in the subsurface region seems to play a role in the simple surface kinetics observed

for these organic molecules on Zr(0001) as compared to the complicated kinetics that we have observed previously for nitrogen-containing species.

ACKNOWLEDGMENT

Acknowldgement is made to the Donors of the American Chemical Society Petroleum Research Fund for partial support of this research.

[1]G. B. Hoflund, D. F. Cox, and R. E. Gilbert, J. Vac. Sci. Technol. A **1**, 1837 (1983).
[2]T. Tanabe and M. Tomita, Surf. Sci. **222**, 333 (1989).
[3]D. A. Asbury, G. B. Hoflund, W. J. Peterson, R. E. Gilbert, and R. A. Outlaw, Surf. Sci. **185**, 213 (1987).
[4]K. Ojima and K. Ueda, Appl. Surf. Sci. **165**, 141 (2000).
[5]Y. C. Kang, D. A. Clauss, and R. D. Ramsier, J. Vac. Sci. Technol. A **19**, 1996 (2001).
[6]Y. C. Kang and R. D. Ramsier, Surf. Sci. **519**, 229 (2002).
[7]Y. C. Kang, M. M. Milovancev, D. A. Clauss, M. A. Lange, and R. D. Ramsier, J. Nucl. Mater. **281**, 57 (2000).
[8]Y. C. Kang and R. D. Ramsier, J. Nucl. Mater. **303**, 125 (2002).
[9]N. Stojilovic, Y. C. Kang, and R. D. Ramsier, Surf. Interface Anal. **33**, 945 (2002).
[10]G. B. Hoflund, G. R. Corallo, D. A. Asbury, and R. E. Gilbert, J. Vac. Sci. Technol. A **5**, 1120 (1987).
[11]J. S. Foord, P. J. Goddard, and R. M. Lambert, Surf. Sci. **94**, 339 (1980).
[12]P. Jakob and D. Menzel, Surf. Sci. **201**, 503 (1988).
[13]W. Braun, G. Held, H.-P. Steinbrueck, C. Stellwag, and D. Menzel, Surf. Sci. **475**, 18 (2001).
[14]H. H. Graen, M. Neuber, M. Neumann, G. Illing, H.-J. Freund, and F.-P. Netzer, Surf. Sci. **223**, 33 (1989).
[15]K. M. E. Habermehl-Cwirzen, J. Katainen, J. Lahtinen, and P. Hautojarvi, Surf. Sci. **507–510**, 57 (2002).
[16]J. R. Lou, P. C. Wong, and K. A. R. Mitchell, Can. J. Chem. **66**, 3157 (1988).